

Multifunctional Protein Nanowire Humidity Sensors for Green Wearable Electronics

Xiaomeng Liu, Tianda Fu, Joy Ward, Hongyan Gao, Bing Yin, Trevor Woodard, Derek R. Lovley, and Jun Yao*

Sustainably produced biomaterials can greatly improve the biocompatibility of wearable sensor technologies while reducing the energy and environmental impacts of materials fabrication and disposal. An electronic sensor device in which the sensing element is a thin ($\approx 2 \mu\text{m}$) film of electrically conductive protein nanowires harvested from the microbe *Geobacter sulfurreducens* is developed. The sensor rapidly responds to changes in humidity with high selectivity and sensitivity. The sensor is integrated on a flexible substrate as a wearable device, enabling real-time monitoring of physiological conditions such as respiration and skin hydration. Noncontact body tracking is demonstrated with an array of sensors that detect a humidity gradient at distance from the skin with high sensitivity. Humidity gradients induce directional charge transport in the protein nanowires films, enabling the production of a current signal without applying an external voltage bias for powerless sensing. These results demonstrate the considerable promise for developing protein nanowire-based wearable sensor devices.

1. Introduction

Electronic sensors are advantageous for wearable applications ranging from energy harvesting, motion control, physiological monitoring, disease diagnostics, to biomedical remedies.^[1–8] Sustainably produced, biocompatible and flexible electrically conductive materials are required for the development of next-generation wearable sensors.^[9–11] Biologically produced materials are especially attractive because they share many properties with biological tissues. For example, silk has been incorporated into various sensing devices.^[10,11] However, silk


lacks native conductivity to be the active conductive element in a conventional sensor structure.

In contrast, the electrically conductive protein nanowires (e-PNs) harvested from the microbe *Geobacter sulfurreducens* are intrinsically conductive.^[12,13] e-PN conductivity can be tuned with genetic modifications to yield a range of conductivities ($\approx 10 \mu\text{S cm}^{-1}$ to 1 kS cm^{-1}) in thin ($\approx 3 \text{ nm}$) wires.^[12,13] e-PN conductivity is highly responsive to pH, with changes of 5000-fold in individual wire conductivity over a range of pH 2–10.5.^[14] These results demonstrate that e-PN conductivity is highly sensitive to changes in surface charge state, a desirable feature for designing sensing capabilities because surface adsorbates often induce a change in surface charge.^[15,16] Although they are comprised of protein, *G. sulfurreducens*

e-PNs are highly robust with stability over a broad pH range (e.g., pH 2–10), at high temperatures ($>100 \text{ }^\circ\text{C}$) and in organic solvents.^[12] Unlike silicon nanowires,^[17,18] e-PNs do not dissolve in physiological fluids. e-PNs can be mass-produced from inexpensive renewable feedstocks without the need for hazardous chemicals in processing and there are no toxic components in the final product.^[12,13] They are fabricated from renewable feedstocks, with energy requirements 100-fold less than for processing silicon.^[19] Thus, e-PNs are a “green” electronic material, with the low-cost, low-energy, and low-waste properties desirable for many dispensable wearable devices.

X. Liu, T. Fu, H. Gao, Dr. B. Yin, Prof. J. Yao
 Department of Electrical and Computer Engineering
 University of Massachusetts
 Amherst, MA 01003, USA
 E-mail: juny@umass.edu

J. Ward, T. Woodard, Prof. D. R. Lovley
 Department of Microbiology
 University of Massachusetts
 Amherst, MA 01003, USA
 Prof. D. R. Lovley, Prof. J. Yao
 Institute for Applied Life Sciences (IALS)
 University of Massachusetts
 Amherst, MA 01003, USA

 The ORCID identification number(s) for the author(s) of this article can be found under <https://doi.org/10.1002/aelm.202000721>.

DOI: 10.1002/aelm.202000721

2. Results

2.1. Basic Device Performance

Here, we report on an initial evaluation of e-PNs as the active sensing component in electronic sensors. We focused on humidity sensing, a common start in the evaluation of new materials for sensor technologies and an important metric related to diverse environments, human activities, and health.^[20–23] For example, humidity sensors play important roles in wearable devices for monitoring body position,^[24,25] respiration,^[20–23] hydration,^[26–28] and wound healing.^[29–31]

The prototype sensor device was fabricated by drop-casting e-PNs harvested from *G. sulfurreducens* onto a pair of

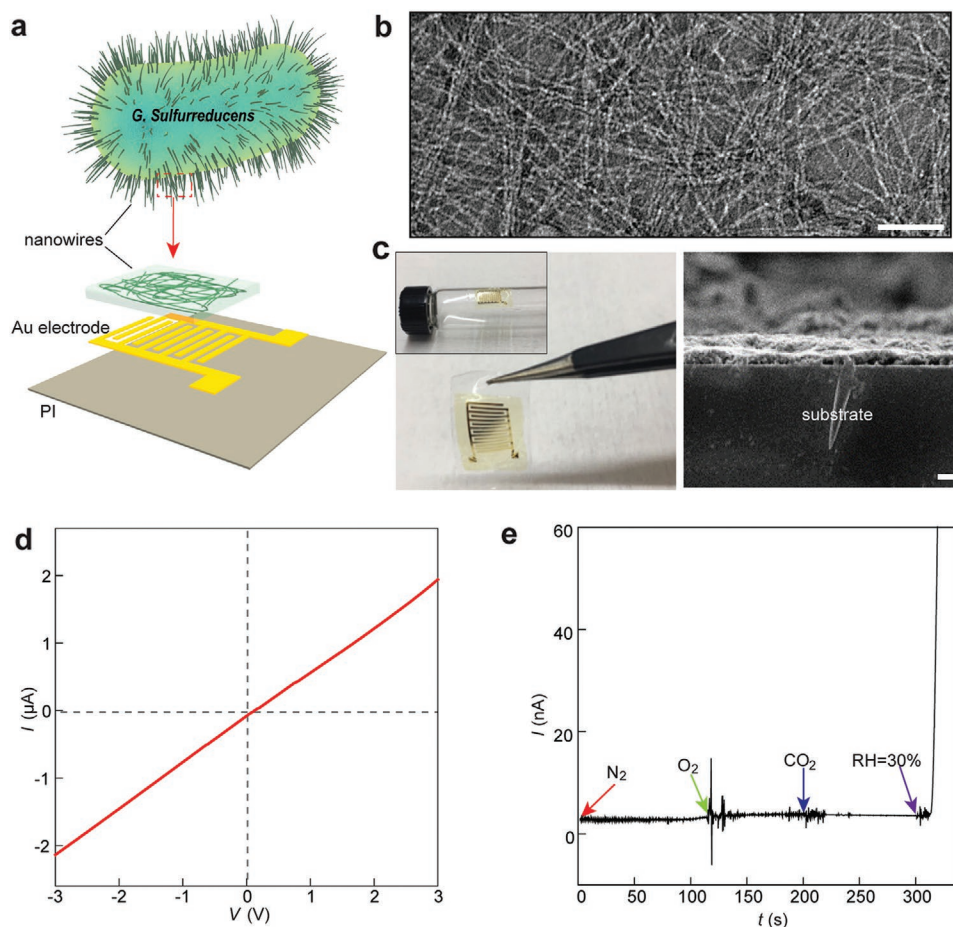


Figure 1. Protein nanowires and devices. a) (Top) Schematic of microorganism *Geobacter sulfurreducens* with outer-membrane protein nanowires, and (bottom) schematic of the sensor device made from harvested protein nanowires. b) TEM images of purified protein nanowires. Scale bar, 100 nm. c) (Left) Fabricated flexible protein nanowire device, which conformally covers on a glass vial (inset). (Right) Cross-section SEM image of the protein nanowire film. Scale bar, 1 μm . d) Representative I - V curve recorded from a protein nanowire device under ambient environment ($\text{RH} \approx 50\%$). e) Current response from a protein nanowire device to atmospheric gases. A voltage bias of 1 V was applied to the device. The baseline current was measured at $\text{RH} \approx 5\%$, so here the relative signal change ($\Delta I/I$) at $\text{RH} = 30\%$ was higher than that in Figure 2a using a baseline current measured at $\text{RH} = 20\%$.

interdigitated Au electrodes patterned on a polyimide (PI) substrate (Figure 1a–c; Figure S1, Materials and Methods, Supporting Information). Scanning electron microscopy (SEM) revealed that the nanowire films were $\approx 2 \mu\text{m}$ thick (Figure 1c). The current–voltage (I - V) response in the ambient environment (Figure 1d) was nearly linear, and passed through the origin, consistent with the ohmic-like response previously observed in e-PN films with a comparable planar device configuration and a pair of symmetric electrodes.^[15] This response contrasts to the previously reported^[32] I - V response observed with a vertical pair of asymmetric electrodes across the film, which yields an I - V curve that does not pass through the origin due to current production that is derived from a vertical moisture gradient within the film. The planar device configuration employed here is not expected to develop an in-plane moisture gradient and hence no electric energy output. This is evident from the observation that the device acted as a conventional resistive sensor with the I - V passing through the origin. There was negligible change in current output when the device was exposed to increased concentrations of air components such as

N_2 , O_2 , and CO_2 (Figure 1e). In contrast, the current increased substantially when the relative humidity (RH) was increased (Figure 1e).

To further quantify the humidity response, the device was exposed to a broad range of RH. Current increased more than two orders of magnitude when the RH was increased from 20% to 95% (Figure 2a). The dependence of sensor response on film thickness was further studied. A trend of increasing response was observed with the decrease in film thickness below 4 μm (Figure S2a, Supporting Information). This is consistent with the general expectation of increasing surface-to-volume ratio in thinner film and hence enhanced sensitivity, which is also observed in other nanomaterials.^[33,34] However, a reverse trend was observed for film thickness $>4 \mu\text{m}$, in which the sensor response increased with the increase in film thickness and saturated at $\approx 8 \mu\text{m}$ (Figure S2b, Supporting Information). This opposite trend can be understood from the depth-dependent adsorption. The bottom interface had reducing moisture adsorption with increasing film thickness, due to the unique chemical and structural properties in protein nanowires.^[32]

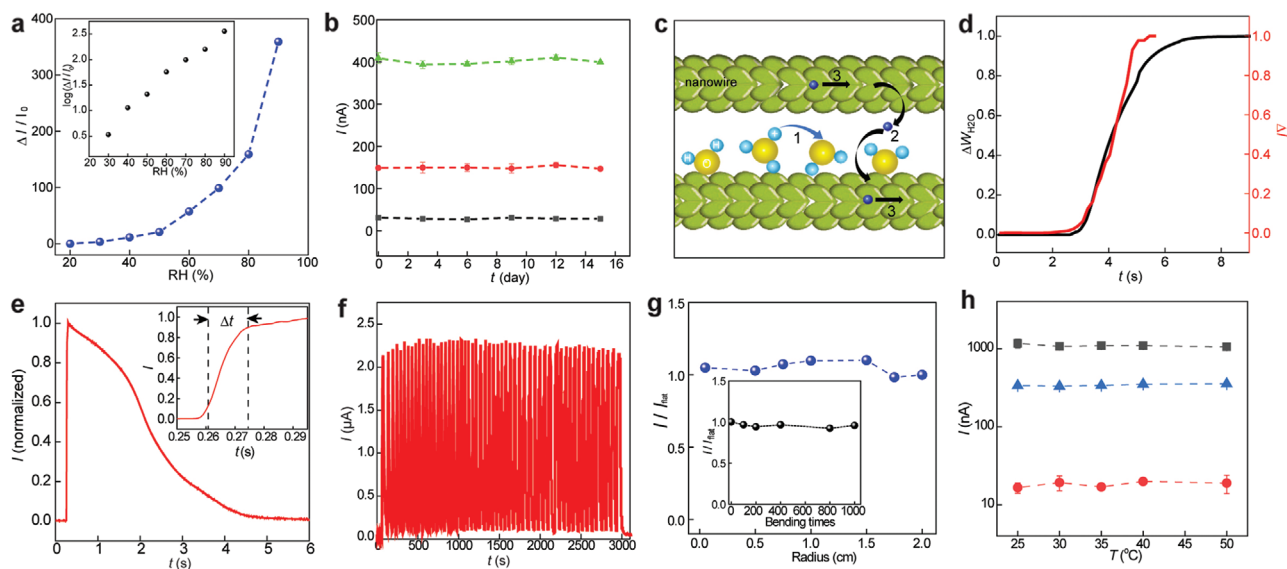


Figure 2. Performance of humidity sensing. a) Relative current change ($\Delta I/I_0$) in the nanowire device with respect to the relative humidity (RH). I_0 is the baseline current measured at RH = 20%. The inset shows the logarithmic scale. b) A half-month continuous measurement of the current (I) in a same device at RH of 40% (gray), 60% (red), and 80% (green). c) Schematic of multiple charge (blue dots) transfer processes contributing to the overall conduction in a protein nanowire film. Path 1, 2, and 3 indicate the general external ionic conduction, interwire conduction, and intrawire conduction, respectively. d) Temporal correlation between moisture adsorption (ΔW_{H_2O} , black curve) in a protein nanowire film and current change (ΔI , red curve) in a nanowire device when RH changed from 30% to 90% by bubbling method (Materials and Methods, Supporting Information). The values are normalized. e) Sensor response to an instant RH change from 30% to 90%. The inset shows the response time (Δt), defined as the rising time from 10% to 90% of the signal peak. f) Sensor response to 55 repeated RH changes from 40% to 90%. g) Sensor current (I) at different bending radii with respect to current (I_{flat}) measured at flat state. (Inset) sensor current in repeated bending test at a bending radius of 0.5 mm. h) Current (I) from a sensor in the temperature range of 25–50 °C, measured at RH of 40% (red), 60% (blue), and 90% (gray). All the data were obtained at a bias of 1 V.

For thick film, this means that the overall sensor resistance is dominated by a layer of high-resistance, moisture-depleted nanowires at the bottom contacts (Figure S2c, Supporting Information), which is evident from the observation that the device resistance actually increased with the increase in film thickness (Figure S2d, Supporting Information). As a result, the increase in thickness effectively increases the average resistivity in the sensor, which is known to generally improve sensitivity in resistive sensors.^[7,35] Importantly, the thickness of $\approx 8 \mu\text{m}$ for the saturation in sensor response (Figure S2d, Supporting Information) coincided with a similar thickness to reach the adsorption depletion at the bottom interface in the protein nanowire film.^[32] This thickness-dependent electrical response in turn provides further evidence for the vertical moisture gradient observed in protein nanowire film.^[32] Overall, the current response is comparable to the highest responses of previously described humidity sensors.^[20–31] Importantly, the sensor maintained a similar level of sensitivity (e.g., $>6\%$ relative conductance change per 1% RH change) across a wide RH range (Figure S3a, Supporting Information), showing the consistent detection capability that was not affected by varied RH baselines in real environment (Figure S3b, Supporting Information). The current response for different RHs was very stable over 15 d (Figure 2b).

Previous studies have demonstrated that e-PN films adsorb moisture from the air.^[32,36,37] Water adsorption in the e-PN devices described here was confirmed with Fourier-transform infrared spectroscopy (Figure S4, Supporting Information).

Quantitative measurements with a quartz crystal microbalance demonstrated that the amount of water adsorbed was dependent on RH (Figure S5, Supporting Information), more water was absorbed at higher RH (Figure S5b, Supporting Information). The amount of water adsorbed was stable over time (Figure S5c, Supporting Information). A likely explanation for the water adsorption capacity of the e-PN films is that the abundant carboxyl and hydroxyl groups confer hydrophilicity to this proteinaceous material. This stable water adsorption (at a stable RH) is the result of a dynamic adsorption–desorption equilibrium,^[32,38,39] which accounts for the dynamic change of adsorption amount in response to RH change (Figure S5b, Supporting Information) and sensor dynamics is further discussed in this context.

Adsorbed water molecules are expected to be ionized and to induce ionization in the high-density functional groups in the protein nanowires.^[32,40] This ionization could enhance the conductivity of e-PN films in several ways (Figure 2c). Most simply, the ionized mobile species will generally contribute to the extrinsic ionic conduction. For example, adsorbed water molecules can form a relay network for proton transport through the Grotthuss mechanism for enhanced conduction.^[40,41] Also, the ionized species are expected to substantially enhance electron transfer between wires within the film. This is important because wire-to-wire resistance appears to be high, as the conductivity of individual e-PNs^[42] is $>10^3$ -fold higher than e-PN films.^[43] Furthermore, water adsorption can modify the surface charge state of diverse materials.^[38,39] The large surface

area and high density of functional groups in e-PNs may enhance this effect. The large impact of “proton doping” on e-PNs conductivity^[14] suggests that surface charge state is an important factor in determining the conduction in individual e-PNs, although the molecular mechanisms warrant further investigation.

There was a close correspondence between the time required for water adsorption in the e-PN films and the current response (Figure 2d), further supporting the suggestion that water adsorption induced a change in conductance of the e-PN films (Figure 2c). There was a very fast response ($\approx 12.7 \pm 2.3$ ms ($n = 3$)) to instant RH change from 30% to 90% (Figure 2e). Decreasing the film thickness (e.g., to 1 μm) further reduced the response time to 7 ms (Figure S6, Supporting Information). This response is among the fastest of known humidity sensors.^[20–31,44] The rapid change of the water adsorption in response to an environmental humidity change indicates that the water in the e-PN film maintains a dynamic equilibrium with the environment. This finding is consistent with the previously documented rapid adsorption–desorption exchange of water molecules at air–solid interfaces.^[32,38,39] When the local RH declined the conductance was rapidly restored to the initial baseline. An increase in the film thickness yielded an increase in both the response time and decay time (Figure S6, Supporting Information), consistent with the expectation of an increasing diffusion time in thicker films. The dynamic response to local RH change was highly repeatable and reproducible (Figure 2f).

2.2. Wearable Implementation

Prototype wearable nanowire sensors were fabricated on a PI layer, further supported by a polydimethylsiloxane (PDMS) substrate that can conform to the body surface (Figures S1 and S7, Materials and Methods, Supporting Information). The nanowire sensor showed negligible conductance change at a bending radius of 0.5 mm (Figure 2g), negligible degradation after repeated bending (inset), and an unchanged dynamic sensing response (Figure S8a, Supporting Information). As a result, it minimized interference from bodily movement such as bending at the finger joint (Figure S8b, Supporting Information). Furthermore, the nanowire sensor was largely insensitive to temperature change at varied humidity levels (Figure 2h). The extrapolated maximal temperature sensitivity (e.g., $<0.5\% \text{ } ^\circ\text{C}^{-1}$) was much smaller than the humidity sensitivity (e.g., $>6\% \text{ RH}^{-1}$, Figure S3a, Supporting Information), indicating that environmental or bodily temperature variation will introduce negligible interference to humidity sensing. Collectively, the protein nanowire sensor showed the potential for wearable detection of bodily humidity for health monitoring and diagnosis.

Therefore, we further investigated wearable sensing of bodily humidity. First, devices placed close to the nose responded to the local RH change created by the breath, providing a real-time monitoring of the respiratory rate (Figure 3a) that increased during exercise compared to a resting state. Second, skin hydration levels can be indicative of various health and disease states.^[26–31] Skin hydration leads to a RH change close

to the skin surface, thus a moisture sensor can also monitor the hydration state.^[26–28] The e-PN-based sensor could detect local RH differences at i) different body locations (Figure 3b) and ii) different body states (Figure 3c). These results demonstrate that the sensor arrays can provide both spatial and temporal mapping of body hydration state for comprehensive diagnostics.

2.3. Noncontact Perception

Orthogonal to the surface distribution of RH, is a vertical RH gradient with RH decreasing as distance from the skin increases. The high sensitivity for RH enabled a dynamic detection of a finger movement above the sensor, in which the translational and vertical distance of the fingertip was inferred through the sensing signal (Figure 3d). Reversing the voltage bias in the sensor yielded a corresponding reversal in the signal signs (Figure S9a, Supporting Information), and wearing a glove reduced the signal to negligible level (Figure S9b, Supporting Information). These controls unambiguously demonstrated that the detection was from skin humidity and not from artifacts (e.g., mechanical perturbation). Quantitative analysis revealed that the nanowire sensor responded to a RH gradient from the finger, with an approximately linear decrease in the sensing signal with the increase in distance from the fingertip (Figure 3e). A finger distance as far as 10 mm was readily detected. Previously, tactile sensors have been integrated in arrays to map pressure distribution and for intelligent object differentiation.^[45,46] By employing a similar concept, the protein nanowire sensors may be used to realize noncontact perception for performance augmentation in intelligent applications (Figure 3f, top left). In a proof-of-concept demonstration with a 4×4 sensor matrix (Figure 3f, bottom left), the relative signal in each sensor reflected its relative position to the fingertip placed above the matrix and these data enabled a reconstruction and location of the fingertip (Figure 3f).

Moisture gradients that form in e-PN films with an asymmetric vertical device structure in the ambient environment yield electric current outputs.^[32] Therefore, it was of interest to determine whether an external humidity/moisture gradient in a symmetric device structure might induce current in an unbiased device. Various energy conversion, harvesting, transmission, and storage strategies have been developed to support the continuous powering of wearable devices,^[2,47–50] because harvesting energy from the environment yields clean and sustainable powering.^[2,51] Humidity carries both electrostatic and kinetic energy that can be converted into electric energy.^[52] Specifically, a moisture gradient in conductive porous materials can either induce an ionization gradient for charge diffusion or nanofluidic water transport that carries charge flow, both of which generate electric current.^[51–54]

2.4. Powerless Sensing

The e-PN films have high-density nanoscale pores or channels for moisture adsorption and transport (Figure S5b, Supporting Information).^[32] The high-density surface functional

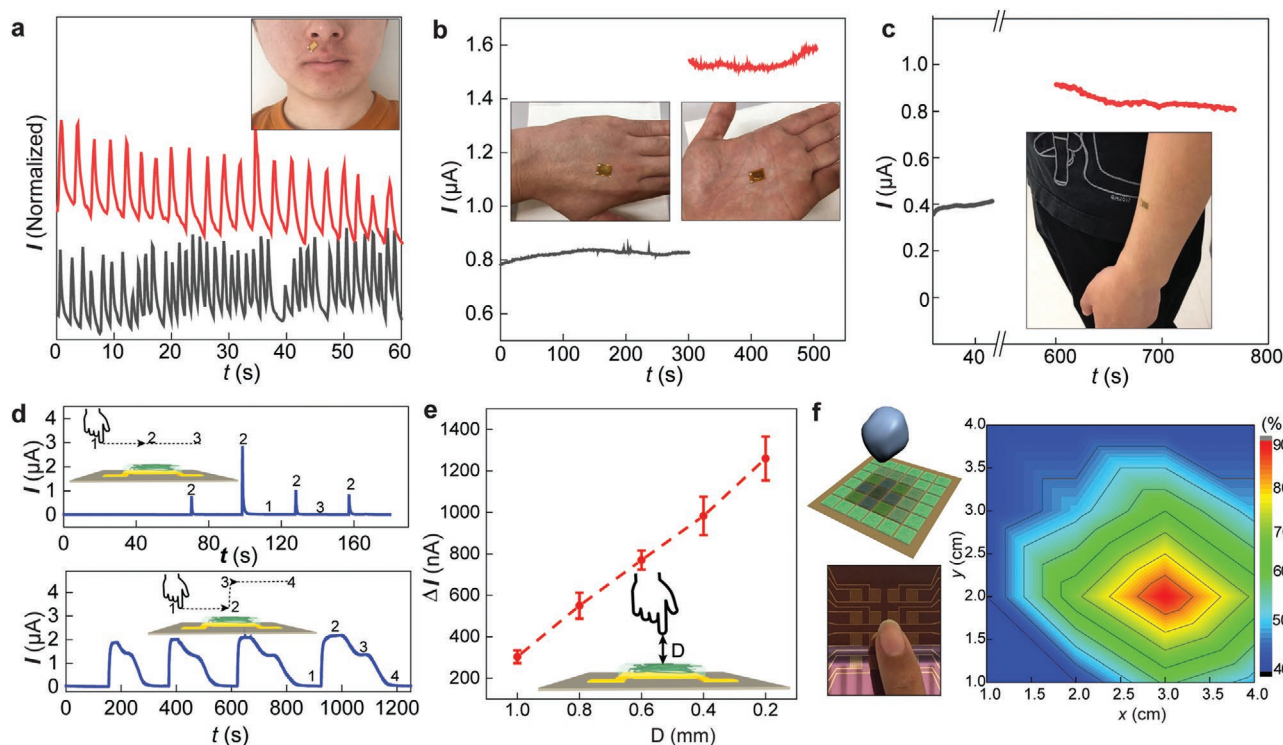


Figure 3. Proof-of-concept implementation of protein nanowire sensors. a) Current responses from a protein nanowire device placed close to the nose, measured at (red) normal state and (gray) after exercise. b) Current responses from a protein nanowire device placed on the hand palm (gray curve) and on the back of the hand (red line). c) Current responses from a protein nanowire device placed on the arm (gray) before and (red) after exercise. d) Current responses from a protein nanowire device to repeated (four times) finger movements of (top) swiping across and (bottom) gradual elevating. The insets show the schematics of finger track, with the numbers indicating the positions. e) The current response in a protein nanowire device with respect to the distance (D) to a vertical fingertip. f) (Top left) Schematic of mapping noncontact objective using nanowire sensor arrays. The moisture adsorption in each sensor unit is relevant to the distance to the objective, which is further converted to current signal. (Bottom left) A proof-of-concept 4×4 nanowire device matrix fabricated on a Si substrate. (Right) Reconstructed contour map of current signal with respect to a noncontact fingertip placed above the matrix.

groups (e.g., carboxyl and hydroxyl) in the nanowires will produce mobile charges (e.g., protons) upon moisture-induced ionization.^[32] If a moisture gradient is induced in the film, the resultant ionization gradient would induce charge diffusion in the mobile species and hence a nonlocal electric current flow (Figure 4a). For example, increasing the humidity gradient in the device plane by rotating the device from a parallel to a perpendicular position to the water surface increased the current signal in an unbiased sensor (Figure 4b).

As moisture-gradient-induced streaming potential can also induce current generation,^[53] we performed additional study to further evaluate the proposed mechanism (Figure 4a). Specifically, streaming current is dependent on the surface charge state or a zeta potential ζ . Changing the sign of surface charge resulted in a sign change in the current.^[55] However, the charge-diffusion mechanism does not predict a sign change in the current (Figure 4a). We therefore varied the surface charge state in protein nanowires by modulating the pH in the preparation solution. Specifically, a low pH (e.g., ≈ 2) and high pH (e.g., ≈ 10) were predicted to introduce positive and negative charges in protein nanowires, respectively.^[56] The control showed that the produced current maintained the same sign independent of modulated surface charge states

(Figure 4c), excluding the streaming mechanism and confirming the diffusion mechanism. In addition, the current direction was consistent with the analysis of charge (H^+) diffusion,^[32] directing from the downstream to the upstream of the moisture gradient. A trend of current increase was observed with the decrease in pH (Figure 4c), which was consistent with previous study showing that a lower pH increased the conductivity in protein nanowires.^[14]

These results demonstrated the potential for powerless sensing of bodily signals. An unbiased nanowire sensor placed close to the nose, where a humidity gradient was anticipated from exhaling, produced a peak current signal ≈ 100 nA with the periodicity matching to the breathing rate (Figure 4d), resulting in self-powered respiratory monitoring. The baseline RH can affect the current output for given humidity gradient between the two electrodes (Figure S10, Supporting Information), which can be readily explained by the RH-dependent device resistance (Figure 2a). Practically, body generally produces a stable range of humidity, thus yielding an instant RH change with fixed peak value; such bodily RH change can also be differentiated from a wide range of ambient RH baselines (Figure S11, Supporting Information). The self-powered humidity sensor can be readily converted to a wearable energy generator to

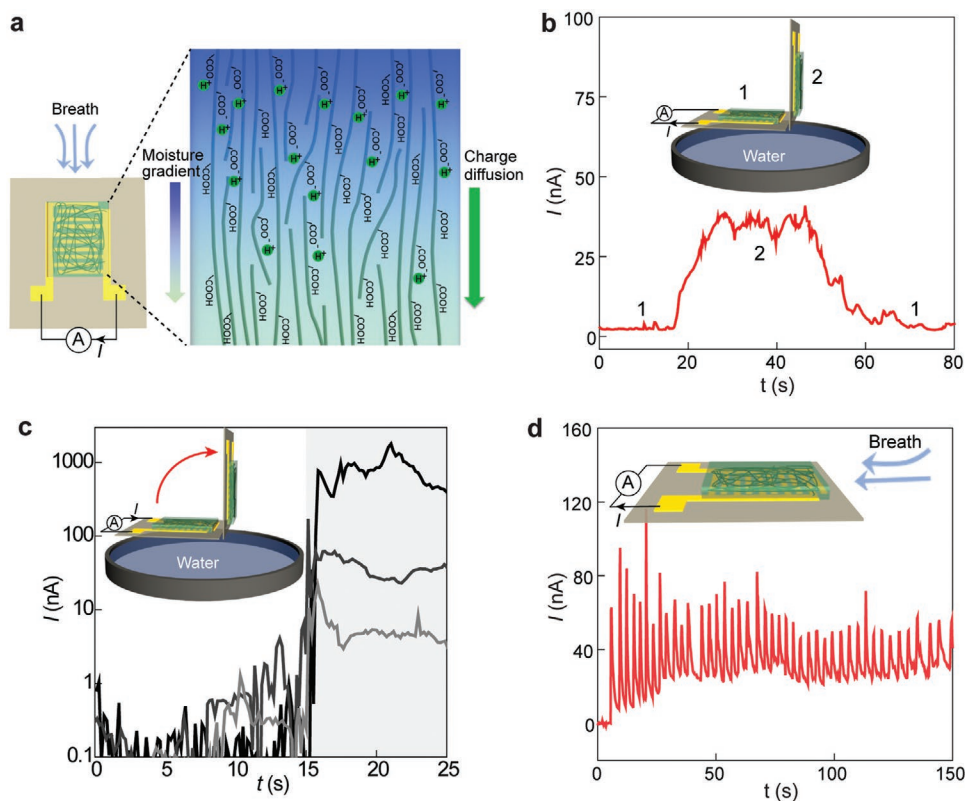


Figure 4. Self-powered sensors. a) Schematic of the current generation in an unbiased protein nanowire device exposed to a humidity gradient (e.g., upon a breath). The humidity gradient induces a moisture-adsorption gradient in the film, which further generates an ionization gradient. The ionization gradient leads to a gradient in the mobile charge species (e.g., protons against an immobile background COOH^-),^[32] which diffuse to generate current. b) A nanowire device placed in a vertical position with respect to the water surface (inset) produced more current than that in a horizontal position. c) Generated currents ($t > 15$) in unbiased protein nanowire sensors by rotating the devices from a horizontal position to vertical position with respect to the water surface (inset). The protein nanowire films were prepared at pH of 2 (black curve), 7 (dark gray), and 10 (gray), respectively. d) An unbiased protein nanowire device served as a self-powered respiratory sensor by converting the humidity gradient of a breath into a current spike.

charge up a capacitor for powering electronics (Figure S12, Supporting Information). Other than chemical doping in nanowires (Figure 4c), structural optimizations in the devices are also expected to improve the power efficiency and continuity, but such exploration is beyond our current focus in the sensor context.

3. Conclusions

In conclusion, we have demonstrated a novel type of electronic sensor made from sustainably produced e-PNs. The high-performance humidity sensing demonstrated here has potential applications in physiological monitoring and remote body tracking with the added possibility of powerless sensing. We expect that the sensing capabilities of e-PN based devices can be expanded to the detection and quantification of a broad range of medically and environmentally significant chemicals/metabolites because the outer surface of e-PNs can be functionalized peptide ligands designed to specifically bind analytes of interest.^[57] Mass production of e-PNs with a specially designed *E. coli* chassis is possible.^[58] Thus, devices

fabricated with e-PNs show substantial potential as a new “green” sensing technology.

Supporting Information

Supporting Information is available from the Wiley Online Library or from the author.

Acknowledgements

J.Y. and D.R.L. acknowledge support from a seed fund through the Office of Technology Commercialization and Ventures at the University of Massachusetts, Amherst. J.Y. acknowledges the support of this work by National Science Foundation (NSF) Awards CBET-1844904 and ECCS-1917630. Part of the device fabrication work was conducted in the clean room of the Center for Hierarchical Manufacturing (CHM), an NSF Nanoscale Science and Engineering Center (NSEC) located at the University of Massachusetts Amherst. Informed consent was obtained from two participants who volunteered to perform these studies (i.e., wearable testing and image publication). All testing reported conformed to the ethical requirements of the University of Massachusetts.

Conflict of Interest

The authors declare no conflict of interest.

Keywords

biomaterials, flexible electronics, green materials, protein nanowires, sensors, wearable devices

Received: July 9, 2020

Published online:

- [1] T. R. Ray, J. Choi, A. J. Bandothkar, S. Krishnan, P. Gutruf, L. Tian, R. Ghaffari, J. A. Rogers, *Chem. Rev.* **2019**, *119*, 5461.
- [2] Z. L. Wang, *ACS Nano* **2013**, *7*, 9533.
- [3] X. Dai, R. Vo, H. H. Hsu, P. Deng, Y. Zhang, X. Jiang, *Nano Lett.* **2019**, *19*, 6658.
- [4] B. Sun, R. N. McCay, S. Goswami, Y. Xu, C. Zhang, Y. Ling, J. Lin, Z. Yan, *Adv. Mater.* **2018**, *30*, 1804327.
- [5] M. G. Stanford, K. Yang, Y. Chyan, C. Kittrell, J. M. Tour, *ACS Nano* **2019**, *13*, 3474.
- [6] C. Wang, X. Li, H. Hu, L. Zhang, Z. Huang, M. Lin, Z. Zhang, Z. Yin, B. Huang, H. Gong, S. Bhaskaran, Y. Gu, M. Makihata, Y. Guo, Y. Lei, Y. Chen, C. Wang, Y. Li, T. Zhang, Z. Chen, A. P. Pisano, L. Zhang, Q. Zhou, S. Xu, *Nat. Biomed. Eng.* **2018**, *2*, 687.
- [7] B. Yin, X. Liu, H. Gao, T. Fu, J. Yao, *Nat. Commun.* **2018**, *9*, 5161.
- [8] H. Lee, T. K. Choi, Y. B. Lee, H. R. Cho, R. Ghaffari, L. Wang, H. J. Choi, T. D. Chung, N. Lu, T. Hyeon, S. H. Choi, D.-H. Kim, *Nat. Nanotechnol.* **2016**, *11*, 566.
- [9] M. Muskovich, C. J. Bettinger, *Adv. Healthcare Mater.* **2012**, *1*, 248.
- [10] B. Zhu, H. Wang, W. R. Leow, Y. Cai, X. J. Loh, M. Y. Han, X. Chen, *Adv. Mater.* **2016**, *28*, 4250.
- [11] H. Tao, M. A. Brenckle, M. Yang, J. Zhang, M. Liu, S. M. Siebert, R. D. Averitt, M. S. Manno, M. C. McAlpine, J. A. Rogers, D. L. Kaplan, F. G. Omenetto, *Adv. Mater.* **2012**, *24*, 1067.
- [12] D. R. Lovley, *Curr. Opin. Electrochem.* **2017**, *4*, 190.
- [13] D. R. Lovley, D. Walker, *Front. Microbiol.* **2019**, *10*, 2078.
- [14] R. Y. Adhikari, N. S. Malvankar, M. T. Tuominen, D. R. Lovley, *RSC Adv.* **2016**, *6*, 8354.
- [15] J. Yao, Z. Jin, L. Zhong, D. Natelson, J. M. Tour, *ACS Nano* **2009**, *3*, 4122.
- [16] X. Duan, Y. Huang, Y. Cui, C. M. Lieber, *Nano Lett.* **2002**, *2*, 487.
- [17] W. Zhou, X. Dai, T.-M. Fu, C. Xie, J. Liu, C. M. Lieber, *Nano Lett.* **2014**, *14*, 1614.
- [18] H. Gao, B. Yin, S. Wu, X. Liu, T. Fu, C. Zhang, J. Lin, J. Yao, *Nano Lett.* **2019**, *19*, 5647.
- [19] D. R. Lovley, *mBio* **2017**, *8*, e00695.
- [20] S. Borini, R. White, D. Wei, M. Astley, S. Haque, E. Spigone, N. Harris, J. Kivioja, T. Ryhanen, *ACS Nano* **2013**, *7*, 11166.
- [21] P. Yasaei, A. Behranginia, T. Foroozan, M. Asadi, K. Kim, F. Khalili-Araghi, A. Salehi-Khojin, *ACS Nano* **2015**, *9*, 9898.
- [22] J.-W. Han, B. Kim, J. Li, M. Meyyappan, *J. Phys. Chem. C* **2012**, *116*, 22094.
- [23] F. Güder, A. Ainla, J. Redston, B. Mosadegh, A. Glavan, T. J. Martin, G. M. Whitesides, *Angew. Chem., Int. Ed.* **2016**, *128*, 5821.
- [24] J. Feng, L. Peng, C. Wu, X. Sun, S. Hu, C. Lin, J. Dai, J. Yang, Y. Xie, *Adv. Mater.* **2012**, *24*, 1969.
- [25] J. Zhao, N. Li, H. Yu, Z. Wei, M. Liao, P. Chen, S. Wang, D. Shi, Q. Sun, G. Zhang, *Adv. Mater.* **2017**, *29*, 1702076.
- [26] T. Li, L. Li, H. Sun, Y. Xu, X. Wang, H. Luo, Z. Liu, T. Zhang, *Adv. Sci.* **2017**, *4*, 1600404.
- [27] A. M. S. Yao, A. Malhotra, F. Lin, A. Bozkurt, J. F. Muth, Y. Zhu, *Adv. Healthcare Mater.* **2017**, *6*, 1601159.
- [28] S. Kano, K. Kim, M. Fujii, *ACS Sens.* **2017**, *2*, 828.
- [29] D. McColl, B. Cartlidge, P. Connolly, *Int. J. Surg.* **2007**, *5*, 316.
- [30] N. Mehmood, A. Hariz, S. Templeton, N. H. Voelcker, *Biomed. Eng. Online* **2015**, *14*, 17.
- [31] T. R. Dargaville, B. L. Farrugia, J. A. Broadbent, S. Pace, Z. Upton, N. H. Voelcker, *Biosens. Bioelectron.* **2013**, *41*, 30.
- [32] X. Liu, H. Gao, J. Ward, X. Liu, B. Yin, T. Fu, J. Chen, D. R. Lovley, J. Yao, *Nature* **2020**, *578*, 550.
- [33] M. Donarelli, L. Ottaviano, *Sensors* **2018**, *18*, 3638.
- [34] S. Cui, H. Pu, P. A. Wells, Z. Wen, S. Mao, J. Chang, M. Hersam, J. Chen, *Nat. Commun.* **2015**, *6*, 8632.
- [35] J. Park, Y. Lee, J. Hong, M. Ha, T.-D. Jung, H. Lim, S. Y. Kim, H. Ko, *ACS Nano* **2014**, *8*, 4689.
- [36] T. Fu, X. Liu, H. Gao, J. E. Ward, X. Liu, B. Yin, Z. Wang, Y. Zhuo, D. J. F. Walker, J. J. Yang, J. Chen, D. R. Lovley, J. Yao, *Nat. Commun.* **2020**, *11*, 1861.
- [37] A. F. Smith, X. Liu, T. L. Woodard, T. Fu, T. Emrick, J. M. Jimenez, D. R. Lovley, J. Yao, *Nano Res.* **2020**, *13*, 1479.
- [38] T. D. R. Ducati, L. H. Simoes, F. Galembeck, *Langmuir* **2010**, *26*, 13763.
- [39] R. F. Gouveia, F. Galembeck, *J. Am. Chem. Soc.* **2009**, *131*, 11381.
- [40] H. C. Bi, K. B. Yin, X. Xie, J. Ji, S. Wan, L. T. Sun, M. Terrones, M. S. Dresselhaus, *Sci. Rep.* **2013**, *3*, 2714.
- [41] T. Miyake, M. Rolandi, *J. Phys. Condens. Matter* **2016**, *28*, 023001.
- [42] Y. Tan, R. Y. Adhikari, N. S. Malvankar, S. Pi, J. E. Ward, T. L. Woodard, K. P. Nevin, Q. Xia, M. T. Tuominen, D. R. Lovley, *Small* **2016**, *12*, 4481.
- [43] N. S. Malvankar, M. Vargas, K. P. Nevin, A. E. Franks, C. Leang, B.-C. Kim, K. Inoue, T. Mester, S. F. Covalla, J. P. Johnson, V. M. Rotello, M. T. Tuominen, D. R. Lovley, *Nat. Nanotechnol.* **2011**, *6*, 573.
- [44] H. Yan, S. Guo, F. Wu, P. Yu, H. Liu, Y. Li, L. Mao, *Angew. Chem., Int. Ed.* **2018**, *57*, 3922.
- [45] S. Sundaram, P. Kellnhofer, Y. Li, J. Y. Zhu, A. Torralba, W. Matusik, *Nature* **2019**, *569*, 698.
- [46] A. Chortos, J. Liu, Z. Bao, *Nat. Mater.* **2016**, *15*, 937.
- [47] L. Li, Q. Zhong, N. D. Kim, G. Ruan, Y. Yang, C. Gao, H. Fei, Y. Li, Y. Ji, J. M. Tour, *Carbon* **2016**, *105*, 260.
- [48] X. Zhang, J. Grajal, J. L. Vazquez-Roy, U. Radhakrishna, X. Wang, W. Chern, L. Zhou, Y. Lin, P.-C. Shen, X. Ji, X. Ling, A. Zubair, Y. Zhang, H. Wang, M. Dubey, J. Kong, M. Dresselhaus, T. Palacios, *Nature* **2019**, *566*, 368.
- [49] Y. Song, S. Chang, S. Gradecak, J. Kong, *Adv. Energy Mater.* **2016**, *6*, 1600847.
- [50] A. J. Bandothkar, J.-M. You, N.-H. Kim, Y. Gu, R. Kumar, A. M. V. Mohan, J. Kurniawan, S. Imani, T. Nakagawa, B. Parish, M. Parthasarathy, P. P. Mercier, S. Xu, J. Wang, *Energy Environ. Sci.* **2017**, *10*, 1581.
- [51] P. D. Mitcheson, in *32nd Annual Int. Conf. IEEE Engineering in Medicine and Biology Society*, Buenos Aires, Argentina **2010**, p. 3432.
- [52] Z. Zhang, X. Li, J. Yin, Y. Xu, W. Fei, M. Xue, Q. Wang, J. Zhou, W. Guo, *Nat. Nanotechnol.* **2018**, *13*, 1109.
- [53] G. Xue, Y. Xu, T. Ding, J. Li, J. Yin, W. Fei, Y. Cao, J. Yu, L. Yuan, L. Gong, J. Chen, S. Deng, J. Zhou, W. Guo, *Nat. Nanotechnol.* **2017**, *12*, 317.
- [54] F. Zhao, Y. Liang, H. H. Cheng, L. Jiang, L. Qu, *Energy Environ. Sci.* **2016**, *9*, 912.
- [55] F. H. J. van der Heyden, D. Stein, C. Dekker, *Phys. Rev. Lett.* **2005**, *95*, 116104.
- [56] N. S. Malvankar, M. Vargas, K. Nevin, P.-L. Tremblay, K. Evans-Lutterodt, D. Nykpanchuk, E. Martz, M. T. Tuominen, D. R. Lovley, *mBio* **2015**, *6*, e00084.
- [57] T. Ueki, D. J. F. Walker, P.-L. Tremblay, K. P. Nevin, J. E. Ward, T. L. Woodard, S. S. Nonnenmann, D. R. Lovley, *ACS Synth. Biol.* **2019**, *8*, 1809.
- [58] T. Ueki, D. J. F. Walker, T. L. Woodard, K. P. Nevin, S. S. Nonnenmann, D. R. Lovley, *ACS Synth. Biol.* **2020**, *9*, 647.